JPET Fast Forward. Published on February 12, 2008 as DOI: 10.1124/jpet.107.134031

JPET #134031

Regulation of De-differentiation and Re-differentiation in Renal Proximal Tubular Cells by the EGF Receptor

Mark A. Hallman, Shougang Zhuang, and Rick G. Schnellmann

Department of Pharmaceutical and Biomedical Sciences and Department of Cellular and Molecular Pharmacology and Experimental Therapeutics, Medical University of South Carolina, 280 Calhoun Street, POB 250140, Charleston, SC 29425 (MAH and RGS)

Department of Medicine, Brown University School of Medicine, 593 Eddy Street, Providence, Rhode Island 02903 (SZ)

Running title: EGF Receptor Regulates Cellular Re-Differentiation

Corresponding author:

Rick G. Schnellmann, PhD

Department of Pharmaceutical and Biomedical Sciences

Medical University of South Carolina

280 Calhoun Street, POB 250140

Charleston, SC 29425

Phone: 843-792-3754

Fax: 843-792-2620

Email: schnell@musc.edu

Manuscript Information:

Text Pages: 27

Figures: 10

Tables: 0

References: 40

Abstract: 240

Introduction: 692

Discussion: 886

Non-standard Abbreviations: renal proximal tubular cells (RPTC)

Section Assignment: Cellular and Molecular

Abstract

Repair of injured renal epithelium is thought to be mediated by surviving renal proximal tubular cells (RPTC) which must de-differentiate to allow the proliferation and migration necessary for epithelial regeneration. RPTC then re-differentiate to restore tubular structure and function. Current models suggest that epidermal growth factor receptor (EGFR) activation is required for de-differentiation characterized by enhanced vimentin expression, decreased N-cadherin expression, spindle morphology, and loss of apical-basal polarity after injury. Because an *in vitro* model of RPTC re-differentiation has not been reported and the mechanism(s) of re-differentiation has not been determined, we used rabbit RPTC in primary cultures to address these issues. H_2O_2 induced the de-differentiated phenotype which persisted >48 hr; re-differentiation occurred spontaneously in the absence of exogenous growth factors after 72–120 hr. Phosphorylation of two tyrosine residues of EGFR increased 12–24 hr, peaked at 24 hr, and declined to basal levels by 48 hr post-injury. EGFR inhibition during de-differentiation restored epithelial morphology and apical-basal polarity and decreased vimentin expression to control levels 24 hr later. Conversely, exogenous EGF addition increased vimentin expression and potentiated spindle morphology. p38 mitogen activated protein kinase (MAPK) and transforming growth factor (TGF)-β receptor inhibitors did not affect re-differentiation after H_2O_2 injury. Similar results were observed in a mechanical injury model. These experiments represent a new model for the investigation of RPTC re-differentiation after acute injury and identify a key regulator of re-differentiation: EGFR, independent of p38 MAPK and the TGF-β receptor.

Introduction

The physiologic role of renal proximal tubular cells (RPTC) engenders their susceptibility to ischemic and toxic injury. However, the proximal tubular epithelium is capable of regeneration, and full recovery is often observed (Cuppage et al., 1972; Houghton et al., 1976). Regeneration is initiated when surviving RPTC sequentially de-differentiate, migrate, and proliferate to restore monolayer confluency (Toback, 1992; Toback et al., 1993; Abbate and Remuzzi, 1996; Molitoris and Marrs, 1999). Finally, regenerated cells re-differentiate to restore RPTC function and structure (Nony and Schnellmann, 2003; Zhuang et al., 2004; Rasbach and Schnellmann, 2006).

After RPTC injury, de-differentiation and re-differentiation processes resemble epithelial-mesenchymal transition (EMT) and mesenchymal-epithelial transition (MET), respectively (Brabletz et al., 2005; Zhuang et al., 2005). The terms EMT and MET indicate the direction of transdifferentiation of cells between the epithelial and mesenchymal phenotypes (Brabletz et al., 2005). RPTC are columnar and cuboidal in nature with adherens junctions that contain, in part, N-cadherin, which are supported by cortical actin rings and contribute to apical-basal polarity (Takeichi, 1991; Prozialeck et al., 2004). During de-differentiation, epithelial cells lose apical-basal polarity, which is characterized by a flattened and elongated morphology, a lack of tight junctions, and reorganization of actin into stress fibers (Hay, 2005). Furthermore, expression of cadherins specific to epithelial differentiation decreases, and the intermediate filament, vimentin, is expressed (Molitoris et al., 1997; Korsching et al., 2005; Zhuang et al., 2005; Zeineldin et al., 2006). During re-differentiation, these mesenchymal markers are lost, epithelial markers return, and physiologic function is restored (Fujigaki et al., 2006).

Unlike many cell lines, primary cultures of rabbit RPTC, cultured under improved conditions (Nowak and Schnellmann, 1995), exhibit aerobic metabolism, are gluconeogenic, and display markers of differentiation similar to those observed *in vivo*. RPTC exhibit cuboidal morphology, are joined by tight

junctions, are polarized with β_1-integrins and Na^+/K^+ ATPase localized to the basolateral membrane, and exhibit low levels of vimentin (Nowak et al., 2000; Nony et al., 2001; Zhuang et al., 2005). Furthermore, cultured in the absence of serum, RPTC recover from various forms of oxidative, toxic, and mechanical injury without the addition of exogenous growth factors (Nowak et al., 1998; Zhuang et al., 2004; Rasbach and Schnellmann, 2006). Thus, they are an excellent model to study autocrine/paracrine-mediated RPTC differentiation and regeneration *in vitro*.

Using this *in vitro* model, we determined that epidermal growth factor receptor (EGFR) activation is a critical step in de-differentiation after oxidant injury. EGFR was activated during the initial 30 min of oxidant exposure and required p38 mitogen activated protein kinase (p38 MAPK) activity (Zhuang et al., 2005; Rasbach and Schnellmann, 2006). Inhibition of either the Rous sarcoma virus homologue gene product (Src), p38 MAPK, or EGFR prevented vimentin expression and fusiform morphology indicating that sequential activation of Src, p38 MAPK, and EGFR mediates de-differentiation of RPTC (Zhuang et al., 2005). These results reveal that EGFR is required for RPTC de-differentiation subsequent to oxidant injury (Okada et al., 1997; Docherty et al., 2006).

Transforming growth factor-β (TGF-β) is a potent stimulus of EMT in RPTC (Okada et al., 1997), and there is evidence that it cooperates with the EGFR axis to regulate differentiation (Okada et al., 1997; Uchiyama-Tanaka et al., 2001; Docherty et al., 2006). Importantly, EGF exacerbates TGF-β-induced EMT in RPTC, possibly by favoring de-differentiation over apoptosis (Okada et al., 1997; Docherty et al., 2006). We have shown that production of TGF-β increases after oxidant exposure in cultured RPTC (Nowak and Schnellmann, 1997), and other studies indicate that TGF-β causes shedding of EGFR agonists from the membrane (Uchiyama-Tanaka et al., 2001). These studies raise the possibility for TGF-β-induced autocrine activation of the EGFR.

Although the EGFR plays a critical role in de-differentiation in regenerating RPTC, the signaling events that trigger re-differentiation are poorly understood because models which allow exploration of the mechanisms of re-differentiation do not exist. Here, we describe, for the first time, a novel model to study RPTC re-differentiation. Furthermore, the use of this model suggests that the primary mechanism for regulating re-differentiation is decreasing EGFR activation.

Methods

Reagents. AG1478 (4-(3-Chloroanilino)-6,7-dimethoxyquinazoline**)**, SB203580 (4-(4-Fluorophenyl)-2-(4-methylsulfinylphenyl)-5-(4-pyridyl)1H-imidazole), SU6656 (2-oxo-3-(4,5,6,7-tetrahydro-1 *H*-indol-2-ylmethylene)-2,3-dihydro-1*H*-indole-5-sulfonic acid dimethylamide), and SB431542 (4-[4-(1,3-benzodioxol-5-yl)-5-(2-pyridinyl)-1H-imidazol -2-yl]benzamide) were purchased from Calbiochem (San Diego, CA). Recombinant human EGF and recombinant human TGF-β_1 were obtained from R&D Systems (Minneapolis, MN). Rhodamine-phalloidin was purchased from Cytoskeleton (Denver, CO). All other chemicals were obtained from Sigma (St. Louis, MO). Antibodies to phospho-EGFR residues (Y845, Y1068, and Y1173) were purchased from Cell Signaling Technology (Danvers, MA). Antibodies to EGFR, vimentin (clone V9), N-Cadherin, GAPDH, and Na^+/K^+ ATPase were obtained from Santa Cruz Biotechnology (Santa Cruz, CA), Sigma, BD Transduction Labs (San Jose, CA), RDI (Concord, MA), and Upstate (Temecula, CA), respectively.

Isolation and culture of renal proximal tubules. Female New Zealand White Rabbits (2 kg) were purchased from Myrtle's Rabbitry (Thomson Station, TN). RPTC were isolated using the iron oxide perfusion method and grown in 6-well or 35-mm tissue culture dishes under improved conditions as previously described (Nowak and Schnellmann, 1996b). The culture medium was a 1:1 mixture of Dulbecco's modified Eagle's medium/Ham's F-12 (without glucose, phenol red, or sodium pyruvate) supplemented with 15 mM HEPES buffer, 2.5 mM L-glutamine, 1 µM pyridoxine HCl, 15 mM sodium bicarbonate, and 6 mM lactate. Hydrocortisone (50 nM), selenium (5 ng/ml), human transferrin (5 µg/ml), bovine insulin (10 nM), and L-ascorbic acid-2-phosphate (50 µM) were added daily to fresh culture medium.

Injury models. Confluent RPTC were used for all experiments. RPTC monolayers were injured with 1 mM H_2O_2 for 5 hr and washed twice with culture medium as previously described (Zhuang and

Schnellmann, 2004). The completion of this wash step was considered time 0 hr for all experiments. Where noted, RPTC were cultured for 24 hr after H_2O_2 exposure to allow de-differentiation to occur before the addition of the EGFR inhibitor AG1478 (10 μM), the p38 inhibitor SB203580 (20 μM), EGF (10 ng/ml), the TGF-β receptor inhibitor SB431542 (5 μM), TGF-β (0.2 ng/ml), or diluent (0.1% DMSO) for an additional 24 hr (48 hr post-injury). SB431542 was added for a 30 min pre-incubation prior to the addition of TGF-β at 24 hr post-injury. For some experiments, RPTC were injured with 1 mM H_2O_2 for 5 hr. At 4 and 12 hr after H_2O_2 removal, RPTC were treated with the src inhibitor SU6656 (10 μM) or diluent (0.1% DMSO) and cells were either lysed or fixed for immunoblot and immunocytochemical analysis. Cell morphology was observed by light microscopy.

Confluent RPTC were swiped with a comb to produce four 2-mm wide linear wounds as previously described (Zhuang et al., 2004). Sham controls were produced by dragging a pick through the media without touching the cell monolayer. RPTC were washed and incubated for 24 hr, after which AG1478 (10 μM), EGF (10 ng/ml), or diluent (0.1% DMSO) was added, and cells were incubated for an additional 24 hr. Morphology and vimentin expression were evaluated by light microscopy and immunocytochemistry, respectively, 24 and 48 hr after wounding.

Immunoblot analysis. RPTC were washed twice with ice-cold phosphate-buffered saline (PBS), scraped into boiling lysis buffer (1% sodium dodecyl sulfate; 1 mM sodium orthovanadate; 10 mM Tris, pH 7.4), and boiled for 5 minutes. Cell membranes were disrupted by sonication for 30 sec. Equal amounts of lysate protein were separated by SDS-PAGE and transferred to PVDF membranes. Membranes were blocked with 5% milk or bovine serum albumin (BSA) overnight at 4 ºC, incubated 1 hr with various primary antibodies (1:1,000), and washed thoroughly with TBST (5 mM Tris Base, 15 mM sodium chloride, 0.1% Tween-20). Secondary detection of primary antibodies was achieved using an appropriate horseradish peroxidase-conjugated secondary antibody (Pierce) for 1 hr.

Chemiluminescence of bound secondary antibody was detected using an AlphaInnotech ChemImager 5500, and densitometry was performed using AlphaEase Software (San Leandro, CA).

Immunoprecipitation. Protein lysates (5 mg) were incubated with 5 µg of antibody overnight at 4 ºC, immunoprecipitated for 3 hr by incubation with 50 µl protein A-sepharose beads (Roche Diagnostics) and washed with PBS. Proteins were eluted by boiling in SDS-PAGE loading buffer. Immunoblot analysis followed as described above.

Microscopy. RPTC were fixed with methanol at -20 ºC (confocal microscopy) or 10% formalin (fluorescence microscopy), permeabilized, blocked with 8% BSA, and incubated with primary antibody or nonspecific IgG control. An Alexafluor 488-conjugated secondary antibody was added, and RPTC were visualized by fluorescence or confocal microscopy. To examine actin, cells were fixed in 10% formalin, permeabilized with 0.1% Triton-X100 in PBS, and blocked with 1% BSA in PBS. Cells were then incubated with phalloidin-rhodamine diluted in blocking solution for 20 min to label F-actin prior to observation by fluorescent microscopy.

Statistical analysis. All data are presented as the mean ± SEM. Cells isolated from the same rabbit represent one experiment (n=1). Means were compared by ANOVA followed by a Student-Newman-Keuls *post hoc* analysis. $P<0.05$ was considered statistically significant.

Results

We monitored RPTC differentiation status after H_2O_2-induced injury using immunoblot analysis to measure N-cadherin and vimentin expression, and light microscopy to observe morphology (Figs. 1 and 2). As reported previously, RPTC were approximately 50–75% confluent 5 hr after H_2O_2-induced injury (time 0) (Zhuang et al., 2005). At this time, bare areas of plastic were exposed at sites of cell sloughing; however, cells surrounding these bare areas maintained their cuboidal morphology. During the next 24–48 hr, single cells with fusiform morphology and prominent filipodia began to migrate into the bare areas. This morphological pattern remained until 72–96 hr after injury at which time the monolayer had nearly reformed, and the repopulating cells became less elongated and more cuboidal. The cell morphology of injured and control cells were similar at 96 and 144 hr post-injury. These studies reveal that RPTC display mesenchymal morphology 24 and 48 hr after oxidant injury, and epithelial morphology returns gradually between 96 and 144 hr.

Vimentin expression in RPTC exposed to H_2O_2 was elevated at 24 hr, remained elevated at 48 hr, decreased at 72 hr, and returned to control levels at 120 hr (Fig. 2). Vimentin in control RPTC did not change over time. N-cadherin expression was present in control RPTC, decreased significantly at 24 hr after H_2O_2 exposure, and remained decreased over the experimental period. In summary, phenotypic markers of de-differentiation, specifically vimentin expression and loss of N-cadherin, occured at 24 and 48 hr coincidentally with the appearance of mesenchymal morphology. Over time, vimentin decreased and epithelial morphology returned, indicating re-differentiation.

Apical-basal polarity is a characteristic of differentiated epithelial cells. To determine the effects of H_2O_2-induced de-differentiation on cell polarity after injury and during regeneration, the basolateral expression of Na^+/K^+ ATPase in RPTC was measured using confocal microscopy. Na^+/K^+ ATPase staining was localized to the basolateral membrane in control RPTC cultures as previously described

(Fig. 3A) (Nowak et al., 2000). At 24 and 48 hr after injury, basolateral Na^+/K^+ ATPase staining decreased and was diffuse (Fig. 3B, C). By 72 hr post-injury, Na^+/K^+ ATPase expression increased and began to re-localize to the basolateral membrane (Fig. 3D). These results reveal that apical-basal polarity is disrupted during increased vimentin staining and mesenchymal RPTC morphology and returns during the loss of vimentin expression and cuboidal morphology.

In previous studies using this model, we showed that the EGFR mediates de-differentiation after H_2O_2 injury to RPTC (Zhuang et al., 2005). However, the mechanism by which re-differentiation occurs has not been determined. To ascertain whether EGFR activation maintains the de-differentiated state, EGFR was inhibited using the EGFR pharmacological inhibitor, AG1478. RPTC were treated with H_2O_2 as described above and de-differentiation was established at 24 hr when AG1478 or diluent was added. Elevated vimentin expression and spindle morphology persisted in injured cells treated with oxidant and diluent 24 hr later (Fig. 4). In contrast, RPTC treated with AG1478 during de-differentiation displayed cuboidal morphology and decreased vimentin expression, similar to uninjured cells. Conversely, RPTC treated with exogenous EGF subsequent to H_2O_2-induced de-differentiation exhibited enhanced vimentin expression, increased numbers of filipodia, and elongated morphology 24 hr later. Diluent and AG1478 alone had no effect on morphology or vimentin expression of uninjured cells. These data reveal that inhibition of EGFR in de-differentiated RPTC decreases vimentin expression and increases cuboidal morphology (re-differentiation), and that EGF exposure of RPTC in a de-differentiated state enhances and extends vimentin expression and elongated morphology. We suggest that EGFR maintains de-differentiation, that the termination of EGFR activation initiates re-differentiation, and that further EGFR activation enhances and extends de-differentiation of RTPC.

We previously showed that p38 MAPK activation is required for EGFR activation and RPTC de-differentiation after oxidative injury (Zhuang et al., 2005; Rasbach and Schnellmann, 2006). There also

is evidence that EGFR mediates TGF-β-induced de-differentiation (Okada et al., 1997; Uchiyama-Tanaka et al., 2001; Uchiyama-Tanaka et al., 2002; Docherty et al., 2006). Thus, we repeated the above experiment using a p38 MAPK inhibitor SB203580, a TGF-β receptor inhibitor SB431542, and TGF-β_1. Treating de-differentiated RPTC with TGF-β_1 for 24 hr enhanced spindle morphology and vimentin expression compared to de-differentiated cells treated with diluent. These TGF-β-induced effects were abrogated to levels similar to de-differentiated cells following treatment with SB431542. We have previously reported that 20 μM SB203580 is sufficient to prevent p38 activation following oxidant injury (Zhuang et al., 2004; Zhuang et al., 2005; Rasbach and Schnellmann, 2006). De-differentiated RPTC treated with SB203580 or SB431542 under the same conditions exhibited vimentin and fusiform morphology similar to de-differentiated RPTC treated with diluent (Fig. 4). SB203580, SB435142, or TGF- β_1 alone had no effect on uninjured RPTC. These data reveal that exogenous TGF-β_1 enhances oxidant-induced de-differentiation while inhibition of p38 or TGF-β receptor activity had no effect on de-differentiated RPTC.

As shown above, Na^+/K^+ ATPase expression is localized to the basolateral membrane in differentiated RPTC and its expression is decreased and diffuse during de-differentiation. Treatment of RPTC with the EGFR receptor inhibitor, AG1478, after H_2O_2-induced de-differentiation increased basolateral membrane localization of Na^+/K^+ ATPase compared to injured RTPC treated with diluent (Fig. 5). De-differentiated cells treated with EGF for 24 hr retained depleted basolateral Na^+/K^+ ATPase expression, similar to cells treated with diluent. Neither AG1478, EGF, nor diluent altered Na^+/K^+ ATPase expression in uninjured cells. Consistent with the findings of decreased vimentin staining and increased cuboidal morphology, EGFR inhibition initiated the return of the apical-basal polarity in de-differentiated RPTC.

Cytoskeletal morphology during de-differentiation and re-differentiation was observed using rhodamine-phalloidin for F-actin staining and fluorescence microscopy. In uninjured cells, actin was arranged in cortical ring structures (Fig 6). De-differentiated RPTC treated with diluent or EGF at 24 hr had stress fibers and lacked cortical rings at 48 hr; however, AG1478 treatment at 24 hr restored cortical ring structure at 48 hr. These results reveal that EGFR inhibition restores epithelial actin morphology in de-differentiated cells, which is consistent with the increased cuboidal morphology and apical basal polarity and decreased vimentin staining observed in the above experiments.

To determine the role of EGFR activation in re-differentiation, EGFR was immunoprecipitated from cell lysates obtained at several time points after H_2O_2 treatment and immunoblotted using antibodies specific for EGFR phosphorylation at tyrosine residues Y845, Y1068, and Y1173. No appreciable change in total EGFR expression was detected under these conditions (Fig. 7). Phosphorylation at all three residues of the EGFR was similar to uninjured cells immediately after treatment with H_2O_2. EGFR became increasingly phosphorylated at Y845 and Y1068 and reached a maximum approximately 24 hr subsequent to injury before returning to control levels at 48 hr (Fig. 7 A–C). These experiments reveal that an increase in EGFR phosphorylation occurs at 24 hr when the mesenchymal phenotype predominates. The phosphorylation was transient, falling to control levels at 48 hr, and preceded re-differentiation.

We previously reported that EGFR activation occurred within 10 min of H_2O_2-induced injury and required Src activation (Zhuang et al., 2005). To determine if Src mediates EGFR activation and the persistence of the de-differentiated phenotype at 48 hr, we evaluated EGFR activation, vimentin expression, and cortical actin staining after the addition of a specific Src inhibitor (SU6656). SU6656 had no effect on EGFR phosphorylation at 24 hr (Fig. 8A) or vimentin expression at 48 hr (Fig. 8B) after oxidant injury. Injured cells treated with SU6656 displayed fewer cellular processes, somewhat less

elongation (Fig. 8B), and increased cortical actin staining (Fig. 9C) compared to diluent-treated de-differentiated cells at 48 hr. These results reveal that EGFR activation and de-differentiation at 48 hr does not require Src. However, between 24 and 48 hr, Src appears to play a role in cellular morphology and actin reorganization.

To determine whether the de-differentiation/re-differentiation observed in the oxidant model occurred in another injury model in the absence of an exogenous oxidant, a mechanical injury model was used as previously described by our laboratory (Counts et al., 1995; Zhuang et al., 2005). At 24 hr after mechanical injury, RPTC adjacent to the wound edge expressed vimentin and elongated morphology (Fig. 9). However, cells peripheral to the wound edge retained epithelial morphology and no appreciable vimentin expression (Fig. 9). These results reveal that de-differentiation does not require decreased cell density or exogenous oxidants and is a common response to both mechanical and oxidant injuries.

The effects of EGFR inhibition on vimentin expression after mechanical injury was examined by adding AG1478 or diluent to RPTC 24 hr after wounding. Vimentin labeling was elevated 24 hr after mechanical injury and remained elevated at 48 hr, albeit to a lesser degree (Fig. 10). Vimentin staining 48 hr after mechanical injury was less than that observed 48 hr after oxidant injury (Fig. 10). In contrast to diluent treated controls, RPTC treated with AG1478 24 hr after mechanical injury did not express vimentin or elongated morphology 24 hr later. Conversely, RPTC treated with exogenous EGF 24 hr after mechanical injury had elevated vimentin staining and increased cell scattering and elongation 24 hr later compared to diluent-treated controls. These experiments reveal that mechanical injury results in reversible de-differentiation of RPTC near the wound, that exogenous EGFR stimulation increases de-differentiaton, and that inhibition of EGFR stimulates re-differentiation.

Discussion

Current evidence suggests that the regeneration of non-injured and sub-lethally injured RPTC is a major mechanism of recovery from acute kidney injury (Lin et al., 2005). Furthermore, various *in vivo* and *in vitro* studies, including our own, have identified the EGFR as the primary mediator of proliferation and migration in regenerating RPTC after various mechanisms of injury (Humes et al., 1989; Coimbra et al., 1990; Nony and Schnellmann, 2003; Zhuang et al., 2004). In addition, we recently reported that the EGFR is also necessary for de-differentiation of RPTC after H_2O_2-induced injury (Zhuang et al., 2005). A critical gap in the literature are studies to address the mechanism(s) of re-differentiation that results in the return of tubular structure and function. Here, we used an H_2O_2-injury model and a model of mechanical injury to demonstrate re-differentiation of RPTC after injury and reveal a critical role for the EGFR in re-differentiation.

The lack of an *in vitro* model of renal re-differentiation has significantly hindered our understanding of RPTC repair and regeneration. With our H_2O_2-induced RPTC de-differentiation model, we observed that de-differentiation persisted beyond 24–48 hr, and that re-differentiation began spontaneously at 72 hr after the removal of H_2O_2 in the absence of exogenous growth factors. The time frame of dedifferentiation and re-differentiation was consistent EGFR activation and inactivation, respectively. De-differentiation was characterized using multiple markers, including vimentin expression, cell elongation, and the loss of N-cadherin and apical-basal polarity. As cells re-differentiated, epithelial morphology returned and was characterized by compact, round, cobblestone morphology. Closer inspection revealed restoration of the cortical actin ring and the return of Na^+/K^+ ATPase to the basolateral membrane. Decrease of vimentin expression to control levels is a phenotypic marker of re-differentiation, and it was consistent with the morphologic markers. To ensure that these observations were not specific to oxidant-induced de-differentiation or extensive cell loss, a mechanical injury model

was used and the same de-differentiation and re-differentiation results were observed. Thus, RPTC undergo de-differentiation and re-differentiation after different injuries through an autocrine/paracrine pathway.

Unlike numerous epithelial cells, N-cadherin predominates in the proximal tubule of humans and several other species, including the rabbit (Nouwen et al., 1993; Prozialeck et al., 2004). Cadherins are an integral part of the adherens junctions which allow membrane compartmentalization and apical-basal polarity (Takeichi, 1991). Despite the return of apical-basal polarity as the RPTC re-differentiated and became confluent, N-cadherin expression did not return during the 144 hr observed. Possibly, N-cadherin expression eventually recovers, but additional studies are needed to understand N-cadherin regulation under these conditions.

The persistence of the de-differentiated phenotype between 24 and 48 hr allowed us to explore the role of several potential signaling pathways in re-differentiation. We previously observed increased EGFR activation within minutes of H_2O_2 addition that was sustained for 2 hr (Zhuang et al., 2005). Here we reveal a second phase of EGFR activation, which peaks at 24 hr and returns to control levels at 48 hr after the removal of H_2O_2. We hypothesize that this second phase of EGFR activation maintains the de-differentiated phenotype, based upon our observation that EGFR phosphorylation returned to basal levels prior to re-differentiation. Adding an EGFR inhibitor at 24 hr initiated re-differentiation that occurred at 48 hr, further supporting this hypothesis. Conversely, the addition of exogenous EGF during de-differentiation, enhanced and extended de-differentiation. Therefore, we suggest that de-differentiation is initiated and maintained by EGFR activation and that re-differentiation is initiated by EGFR inactivation.

The mechanism responsible for the second phase of EGFR activation is unknown. Src-mediated p38 activation within the first several minutes of oxidant injury is responsible for activating the EGFR to

initiate de-differentiation in this model (Zhuang et al., 2005). In contrast, inhibition of Src or p38 MAPK did not stimulate re-differentiation. Therefore, the mechanism of the second phase of EGFR activation differs from the mechanism that initiates it, and neither Src nor p38 acts downstream of the EGFR to initiate re-differentiation after oxidant injury.

Several possibilities exist for the initiation of the second phase of EGFR activation. For example, EGFR activation may the result of autocrine/paracrine release of EGFR ligands. In this case, stimuli such as hepatocyte growth factor, lysophosphatidic acid, angiotensin II, bradykinin, and prostaglandin E2 may activate membrane-bound sheddases causing the autocrine release of HB-EGF or other EGFR ligands (Liu and Armant, 2004; Schafer et al., 2004; Thomas et al., 2006; Xu and Yu, 2007). It is also possible that the EGFR is transactivated by a mechanism independent of EGFR ligand production. Finally, several protein tyrosine phosphatases (ie PTP1B and TC-PTP) can negatively regulate EGFR activation (Ostman et al., 2006). Inactivation of these phosphatases could also contribute to increased EGFR activity during de-differentiation.

TGF-β is a known stimulus of de-differentiation in many models of epithelial EMT, and its effects are potentiated by EGF (Okada et al., 1997; Docherty et al., 2006). Previous studies indicate that RPTC produce TGF-β after oxidant injury, and at a concentration of 0.2 ng/ml exogenous TGF-β_1 induces glycolytic metabolism, decreased Na^+/K^+ ATPase activity, and cell rounding and detachment (Nowak and Schnellmann, 1996a; Nowak and Schnellmann, 1997). Whereas the current experiments revealed that exogenous TGF-β enhances de-differentiation, TGF-β receptor inhibition had no effect on re-differentiation. Therefore, we suggest that autocrine/paracrine TGF-β signaling does not maintain de-differentiation or mediate re-differentiation under these conditions.

Acknowledgements

The authors thank the MUSC Center for Cell Death, Injury and Regeneration for assistance with confocal microscopy.

References

Abbate M and Remuzzi G (1996) Acceleration of recovery in acute renal failure: from cellular mechanisms of tubular repair to innovative targeted therapies. *Ren Fail* **18**:377-388.

Brabletz T, Hlubek F, Spaderna S, Schmalhofer O, Hiendlmeyer E, Jung A and Kirchner T (2005) Invasion and metastasis in colorectal cancer: epithelial-mesenchymal transition, mesenchymal-epithelial transition, stem cells and beta-catenin. *Cells Tissues Organs* **179**:56-65.

Coimbra TM, Cieslinski DA and Humes HD (1990) Epidermal growth factor accelerates renal repair in mercuric chloride nephrotoxicity. *Am J Physiol* **259**:F438-443.

Counts RS, Nowak G, Wyatt RD and Schnellmann RG (1995) Nephrotoxicant inhibition of renal proximal tubule cell regeneration. *Am J Physiol* **269**:F274-281.

Cuppage FE, Chiga M and Tate A (1972) Cell cycle studies in the regenerating rat nephron following injury with mercuric chloride. *Lab Invest* **26**:122-126.

Docherty NG, O'Sullivan OE, Healy DA, Murphy M, O'Neill A J, Fitzpatrick JM and Watson RW (2006) TGF-beta1-induced EMT can occur independently of its proapoptotic effects and is aided by EGF receptor activation. *Am J Physiol Renal Physiol* **290**:F1202-1212.

Fujigaki Y, Goto T, Sakakima M, Fukasawa H, Miyaji T, Yamamoto T and Hishida A (2006) Kinetics and characterization of initially regenerating proximal tubules in S3 segment in response to various degrees of acute tubular injury. *Nephrol Dial Transplant* **21**:41-50.

Hay ED (2005) The mesenchymal cell, its role in the embryo, and the remarkable signaling mechanisms that create it. *Dev Dyn* **233**:706-720.

Houghton DC, Hartnett M, Campbell-Boswell M, Porter G and Bennett W (1976) A light and electron microscopic analysis of gentamicin nephrotoxicity in rats. *Am J Pathol* **82**:589-612.

Humes HD, Cieslinski DA, Coimbra TM, Messana JM and Galvao C (1989) Epidermal growth factor enhances renal tubule cell regeneration and repair and accelerates the recovery of renal function in postischemic acute renal failure. *J Clin Invest* **84**:1757-1761.

Korsching E, Packeisen J, Liedtke C, Hungermann D, Wulfing P, van Diest PJ, Brandt B, Boecker W and Buerger H (2005) The origin of vimentin expression in invasive breast cancer: epithelial-mesenchymal transition, myoepithelial histogenesis or histogenesis from progenitor cells with bilinear differentiation potential? *J Pathol* **206**:451-457.

Lin F, Moran A and Igarashi P (2005) Intrarenal cells, not bone marrow-derived cells, are the major source for regeneration in postischemic kidney. *J Clin Invest* **115**:1756-1764.

Liu Z and Armant DR (2004) Lysophosphatidic acid regulates murine blastocyst development by transactivation of receptors for heparin-binding EGF-like growth factor. *Exp Cell Res* **296**:317-326.

Molitoris BA, Leiser J and Wagner MC (1997) Role of the actin cytoskeleton in ischemia-induced cell injury and repair. *Pediatric Nephrology* **V11**:761-767.

Molitoris BA and Marrs J (1999) The role of cell adhesion molecules in ischemic acute renal failure. *Am J Med* **106**:583-592.

Nony PA, Nowak G and Schnellmann RG (2001) Collagen IV promotes repair of renal cell physiological functions after toxicant injury. *Am J Physiol Renal Physiol* **281**:F443-453.

Nony PA and Schnellmann RG (2003) Mechanisms of Renal Cell Repair and Regeneration after Acute Renal Failure, in pp 905-912.

Nouwen EJ, Dauwe S, van der Biest I and De Broe ME (1993) Stage- and segment-specific expression of cell-adhesion molecules N-CAM, A-CAM, and L-CAM in the kidney. *Kidney Int* **44**:147-158.

Nowak G, Aleo MD, Morgan JA and Schnellmann RG (1998) Recovery of cellular functions following oxidant injury. *Am J Physiol* **274**:F509-515.

Nowak G, Carter CA and Schnellmann RG (2000) Ascorbic acid promotes recovery of cellular functions following toxicant-induced injury. *Toxicol Appl Pharmacol* **167**:37-45.

Nowak G and Schnellmann RG (1995) Improved culture conditions stimulate gluconeogenesis in primary cultures of renal proximal tubule cells. *Am J Physiol* **268**:C1053-1061.

Nowak G and Schnellmann RG (1996a) Autocrine production and TGF-beta 1-mediated effects on metabolism and viability in renal cells. *Am J Physiol* **271**:F689-697.

Nowak G and Schnellmann RG (1996b) L-ascorbic acid regulates growth and metabolism of renal cells: improvements in cell culture. *Am J Physiol* **271**:C2072-2080.

Nowak G and Schnellmann RG (1997) Renal cell regeneration following oxidant exposure: inhibition by TGF-beta1 and stimulation by ascorbic acid. *Toxicol Appl Pharmacol* **145**:175-183.

Okada H, Danoff TM, Kalluri R and Neilson EG (1997) Early role of Fsp1 in epithelial-mesenchymal transformation, in pp F563-574.

Ostman A, Hellberg C and Bohmer FD (2006) Protein-tyrosine phosphatases and cancer. *Nat Rev Cancer* **6**:307-320.

Prozialeck WC, Lamar PC and Appelt DM (2004) Differential expression of E-cadherin, N-cadherin and beta-catenin in proximal and distal segments of the rat nephron. *BMC Physiol* **4**:10.

Rasbach KA and Schnellmann RG (2006) Signaling of mitochondrial biogenesis following oxidant injury. *J Biol Chem*.

Schafer B, Marg B, Gschwind A and Ullrich A (2004) Distinct ADAM metalloproteinases regulate G protein-coupled receptor-induced cell proliferation and survival. *J Biol Chem* **279**:47929-47938.

Takeichi M (1991) Cadherin cell adhesion receptors as a morphogenetic regulator. *Science* **251**:1451-1455.

Thomas SM, Bhola NE, Zhang Q, Contrucci SC, Wentzel AL, Freilino ML, Gooding WE, Siegfried JM, Chan DC and Grandis JR (2006) Cross-talk between G protein-coupled receptor and epidermal growth factor receptor signaling pathways contributes to growth and invasion of head and neck squamous cell carcinoma. *Cancer Res* **66**:11831-11839.

Toback FG (1992) Regeneration after acute tubular necrosis. *Kidney Int* **41**:226-246.

Toback FG, Kartha S and Walsh-Reitz MM (1993) Regeneration of kidney tubular epithelial cells. *Clin Investig* **71**:861-866.

Uchiyama-Tanaka Y, Matsubara H, Mori Y, Kosaki A, Kishimoto N, Amano K, Higashiyama S and Iwasaka T (2002) Involvement of HB-EGF and EGF receptor transactivation in TGF-beta-mediated fibronectin expression in mesangial cells. *Kidney Int* **62**:799-808.

Uchiyama-Tanaka Y, Matsubara H, Nozawa Y, Murasawa S, Mori Y, Kosaki A, Maruyama K, Masaki H, Shibasaki Y, Fujiyama S, Nose A, Iba O, Hasagawa T, Tateishi E, Higashiyama S and Iwasaka T (2001) Angiotensin II signaling and HB-EGF shedding via metalloproteinase in glomerular mesangial cells. *Kidney Int* **60**:2153-2163.

Xu KP and Yu FS (2007) Cross talk between c-Met and epidermal growth factor receptor during retinal pigment epithelial wound healing. *Invest Ophthalmol Vis Sci* **48**:2242-2248.

Zeineldin R, Rosenberg M, Ortega D, Buhr C, Chavez MG, Stack MS, Kusewitt DF and Hudson LG (2006) Mesenchymal transformation in epithelial ovarian tumor cells expressing epidermal growth factor receptor variant III. *Mol Carcinog* **45**:851-860.

Zhuang S, Dang Y and Schnellmann RG (2004) Requirement of the epidermal growth factor receptor in renal epithelial cell proliferation and migration. *Am J Physiol Renal Physiol* **287**:F365-372.

Zhuang S and Schnellmann RG (2004) H2O2-induced transactivation of EGF receptor requires Src and mediates ERK1/2, but not Akt, activation in renal cells. *Am J Physiol Renal Physiol* **286**:F858-865.

Zhuang S, Yan Y, Han J and Schnellmann RG (2005) p38 kinase-mediated transactivation of the epidermal growth factor receptor is required for dedifferentiation of renal epithelial cells after oxidant injury. *J Biol Chem* **280**:21036-21042.

Footnotes

Funding was provided by NIH F30 ES013619. This work was conducted in a facility constructed with support from the National Institutes of Health, Grant Number C06 RR015455 from the Extramural Research Facilities Program of the National Center for Research Resources.

Legends for Figures

Figure 1. ***Morphology of regenerating RPTC cultures.*** Confluent RPTC were treated with 1 mM H_2O_2 for 5 hr. Cells were washed, and this was designated time 0 hr for the experiment. Control cells were uninjured. Morphology was observed at 24-hr intervals for 6 days. Representative micrographs from 3 experiments.

Figure 2. ***Expression of differentiation markers in regenerating RPTC.*** Confluent RPTC were treated with 1 mM H_2O_2 or diluent for 5 hr. Cells were washed, and this was designated time 0 hr for the experiment. Cell lysates were collected every 24 hr for 6 days and immunoblotted for N-cadherin, vimentin, and GAPDH. Representative blots are shown along with densitometric analysis**. * indicates a statistically significant difference from time-matched controls ($p<0.05$, N=6).**

Figure 3. ***Basolateral Na^+/K^+ ATPase expression after oxidant injury.*** Confluent RPTC were treated with H_2O_2 or diluent and allowed to regenerate. Cells were fixed 24, 48, and 72 hr after oxidant removal. Na^+/K^+ ATPase was labeled by immunocytochemistry, and basolateral membranes were imaged by confocal microscopy. Panel **A** depicts control cells. RPTC 24, 48, and 72 hr after injury are depicted in panels **B**, **C**, and **D**, respectively. Representative micrographs from 3 experiments.

Figure 4. ***Vimentin expression in de-differentiated RPTC treated with pharmacologic inhibitors.*** RPTC were treated with diluent or de-differentiated by H_2O_2-induced injury followed by an additional 24 hr of incubation. The following compounds: 0.1 % DMSO vehicle, 10 μM AG1478, 10 ng/ml EGF, 20 μM SB203580, 5 μM SB431542 or 0.2 ng/ml TGF-β were added for an additional 24 hr. Vimentin was labeled by immunocytochemistry and examined by fluorescent microscopy. Representative micrographs from 5 experiments.

Figure 5. ***Basolateral Na^+/K^+ ATPase expression in regenerating RPTC.*** RPTC were treated with diluent or de-differentiated by H_2O_2-induced injury followed by an additional 24 hr of incubation. The

following compounds were added for an additional 24 hr: 0.1 % DMSO vehicle, 10 μM AG1478, or 10 ng/ml EGF. Na^+/K^+ ATPase was labeled by immunocytochemistry, and basolateral membranes were imaged by confocal microscopy. Representative micrographs 3 experiments.

Figure 6. ***Cytoskeletal morphology in de-differentiated RPTC cultures.*** Confluent RPTC were treated with diluent or 1 mM H_2O_2 for 5 hr and then incubated for 24 hr. AG1478 (10 μM), EGF (10 ng/ml) or diluent (0.1% DMSO) was then added for an additional 24 hr. F-actin was labeled with phalloidin-rhodamine. Examples of stress fiber formation are noted with white arrows. Representative micrographs from 3 experiments.

Figure 7. ***EGFR Phosphorylation in regenerating RPTC.*** Confluent RPTC were treated with 1 mM H_2O_2 or diluent for 5 hr and then incubated for 0, 12, 24, 36 and 48 hr. EGFR was immunoprecipitated from lysates collected at the indicated times. Phosphorylation of EGFR (**A**) Y845 (**B**) Y1068, and (**C**) Y1173 was measured by immunoblot analysis. Representative blots are shown along with densitometric analysis of EGFR phosphorylation at 24 hr. An asterisk (*) indicates statistically significant difference from control RPTC. ($p<0.05$, N=3)

Figure 8: ***EGFR phosphorylation and vimentin expression in de-differentiated RPTC following Src inhibition.*** Confluent RPTC were treated with diluent or 1 mM H_2O_2 for 5 hr. 10 μM SU6656 or diluent (0.1% DMSO) was added at 12 hr after the completion of oxidant injury. Some cells were lysed at 24 hr, lysates were enriched for EGFR by immunoprecipitation and then immunoblotted (A). Remaining cells were fixed at 48 hrs for microscopy. Vimentin was labeled with FITC by immunocytochemistry (B). F-actin was labeled with phalloidin- rhodamine (C).

Figure 9. ***Vimentin expression in mechanically injured RPTC.*** Confluent RPTC were scraped, washed and incubated for 24 hr. Vimentin was labeled by immunocytochemistry and examined by fluorescent microscopy. Representative micrographs from 3 experiments.

Figure 10. ***Vimentin expression in mechanically and oxidant injured RPTC.*** Cells were injured with H_2O_2 or scraped, washed and incubated for 24 hr. Some cultures were incubated an additional 24 hr with AG1478, EGF or diluent (0.1% DMSO). Vimentin was labeled at 24 or 48 hr and examined by fluorescent microscopy. Representative micrographs from 3 experiments.

Figure 1

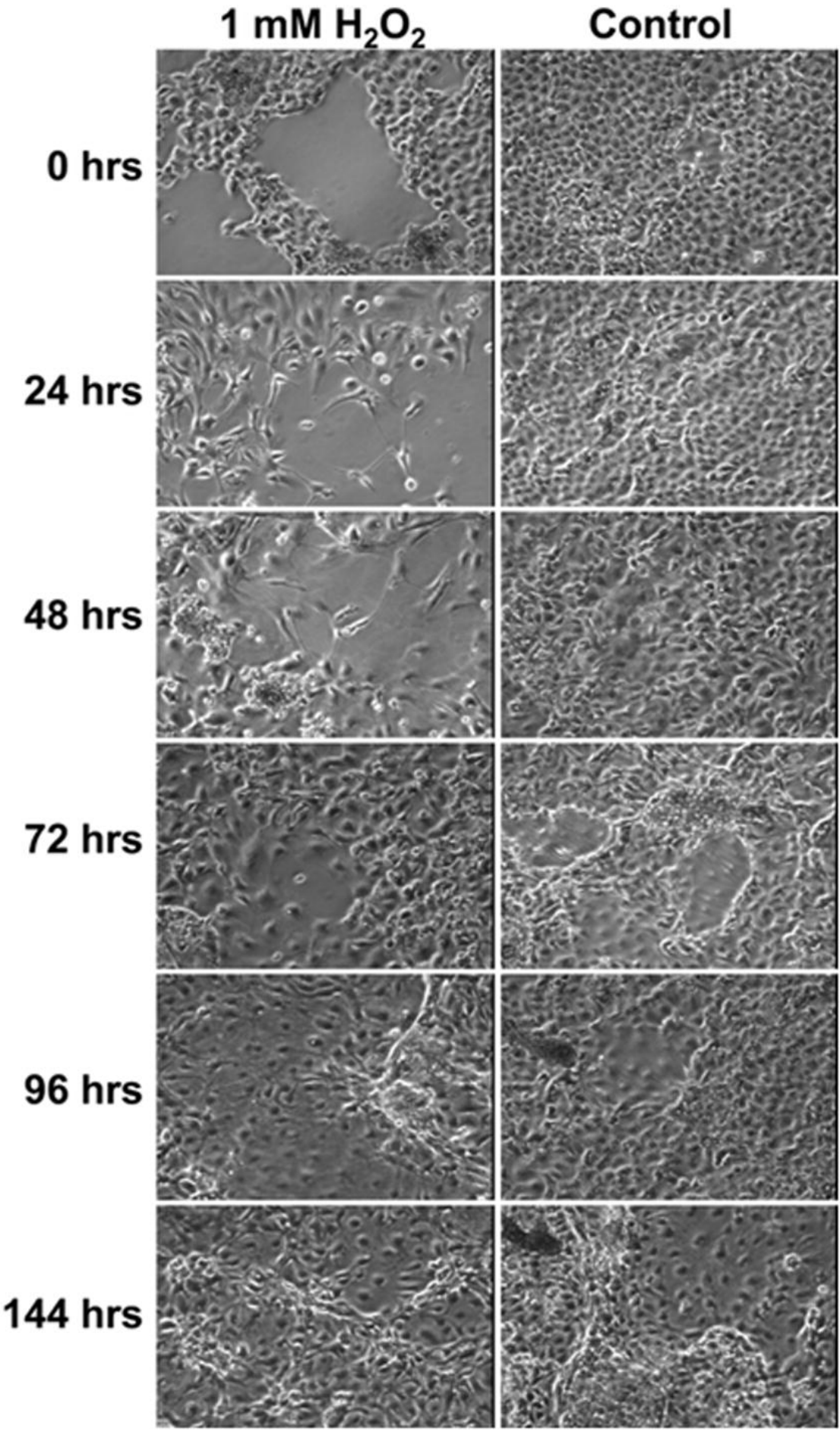

Figure 2

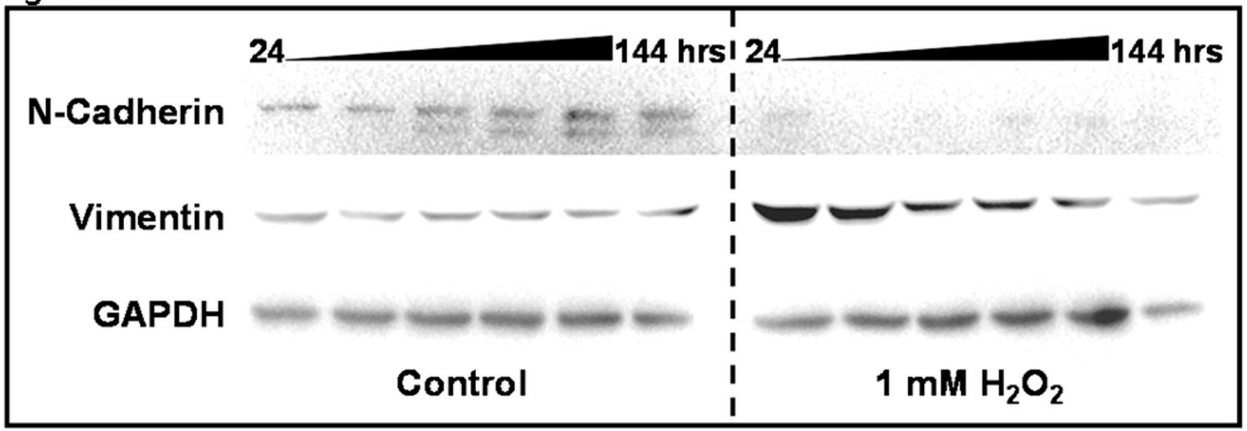
24
144 hrs
24
144 hrs
N-Cadherin
Vimentin
GAPDH
Control
1 mM H_2O_2

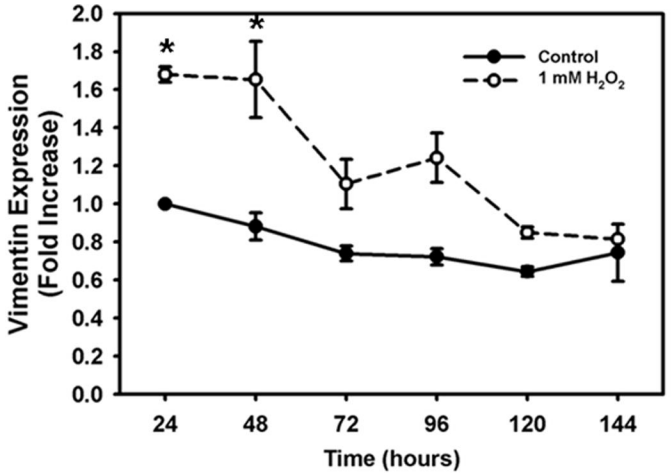
Vimentin Expression
(Fold Increase)
Control
1 mM H_2O_2
Time (hours)
0.0
0.2
0.4
0.6
0.8
1.0
1.2
1.4
1.6
1.8
2.0
24
48
72
96
120
144
*
*

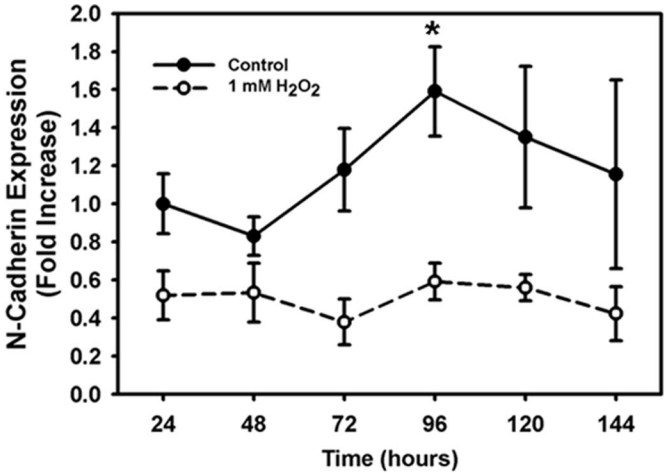
N-Cadherin Expression
(Fold Increase)
Control
1 mM H_2O_2
Time (hours)
0.0
0.2
0.4
0.6
0.8
1.0
1.2
1.4
1.6
1.8
2.0
24
48
72
96
120
144
*

Figure 3

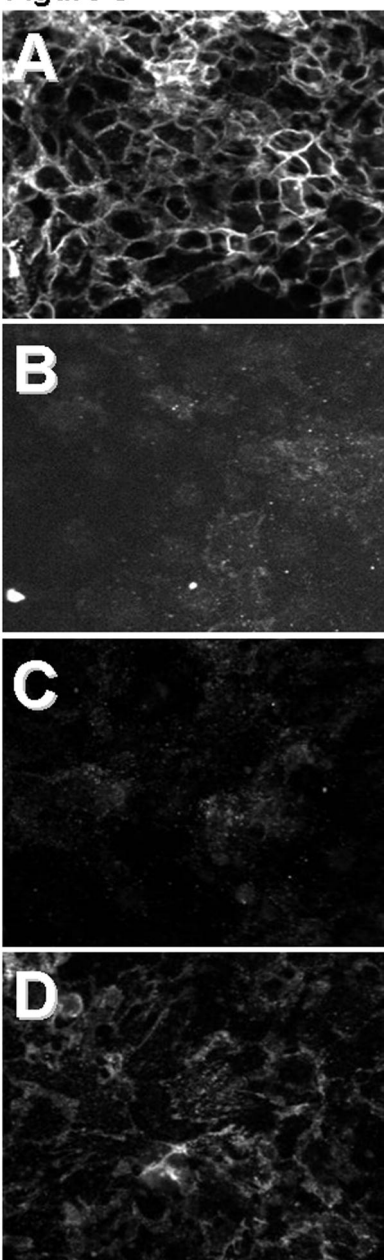

Figure 4

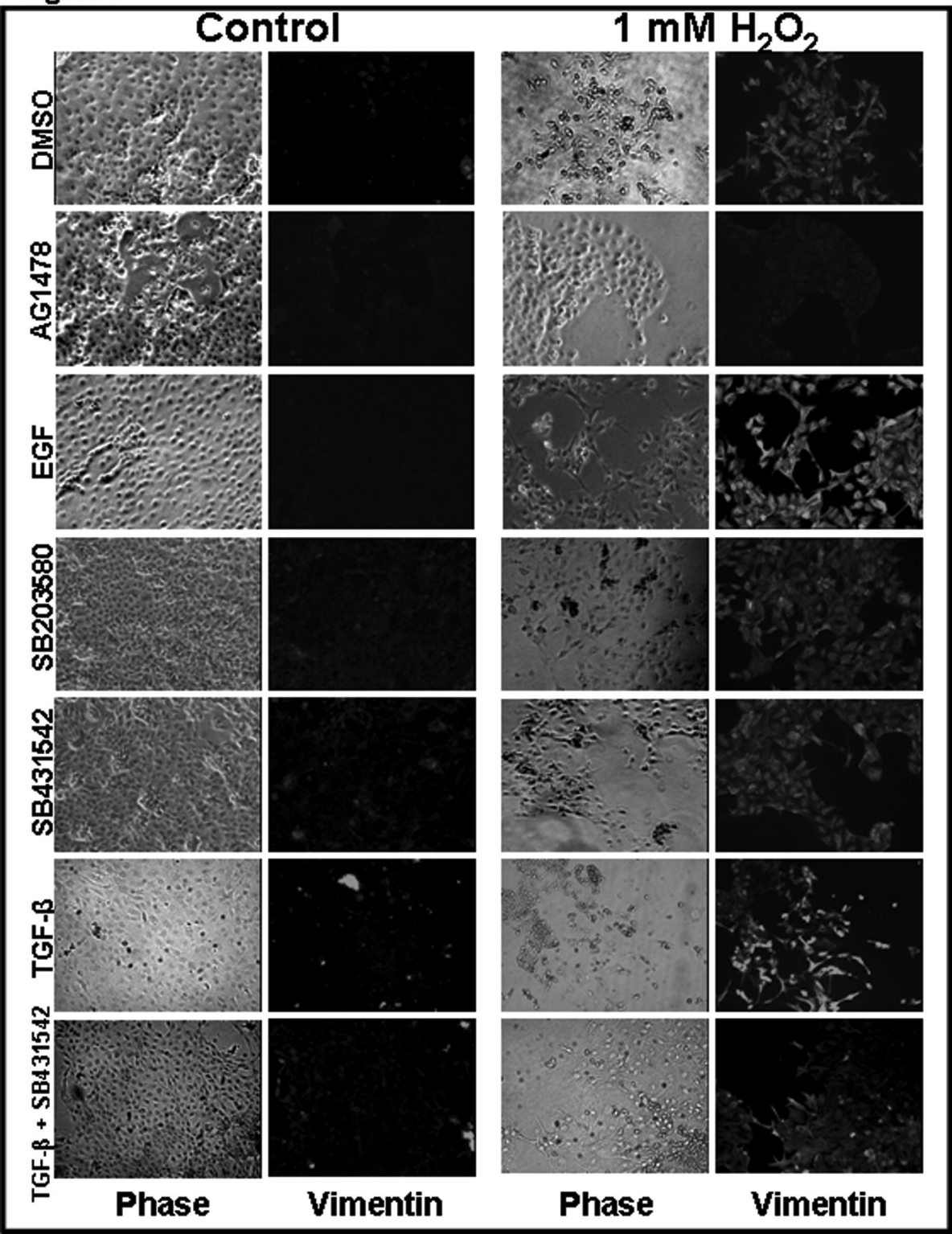
Control
1 mM H_2O_2
DMSO
AG1478
EGF
SB203580
SB431542
TGF-β
TGF-β + SB431542
Phase
Vimentin
Phase
Vimentin

Figure 5

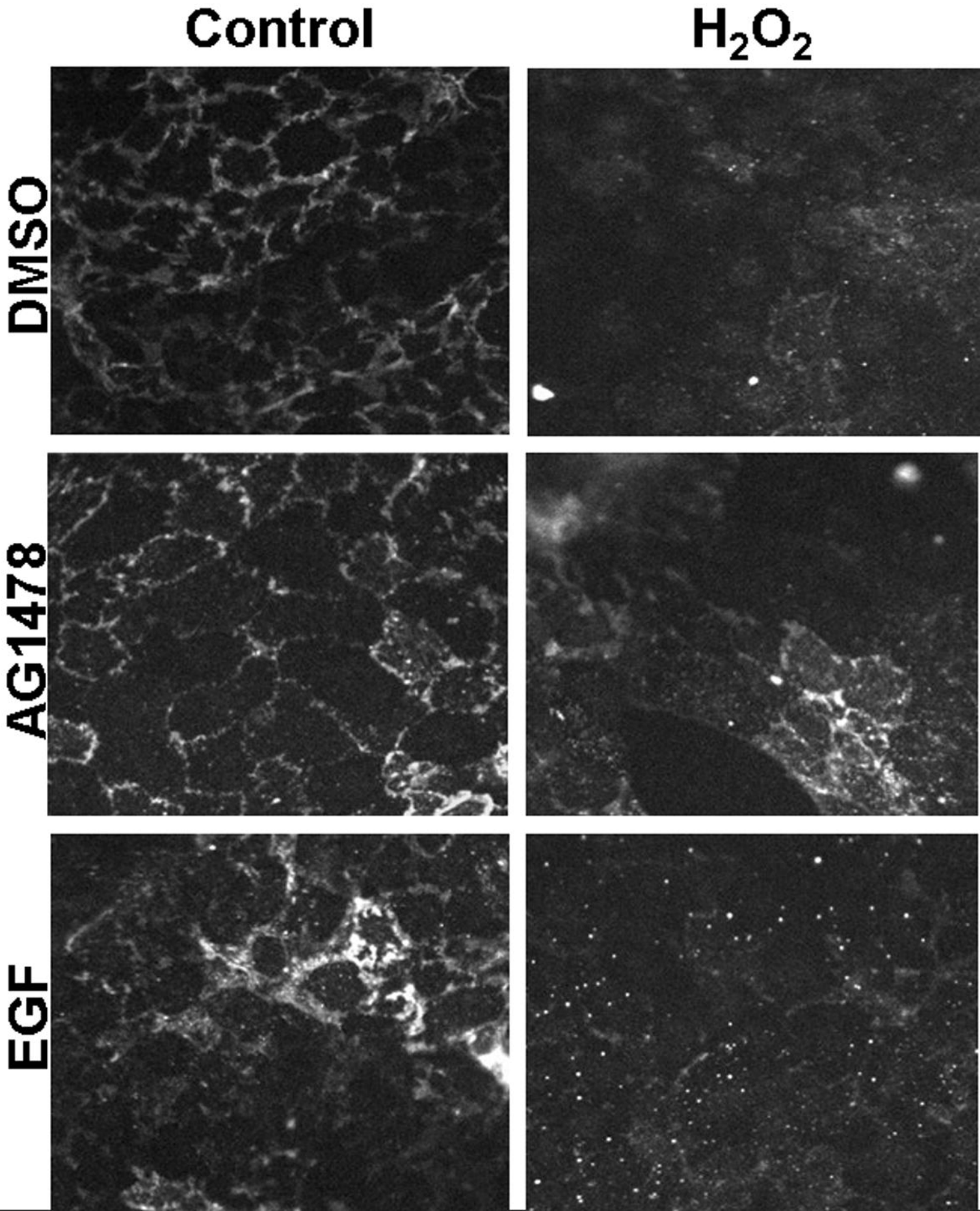

Figure 6

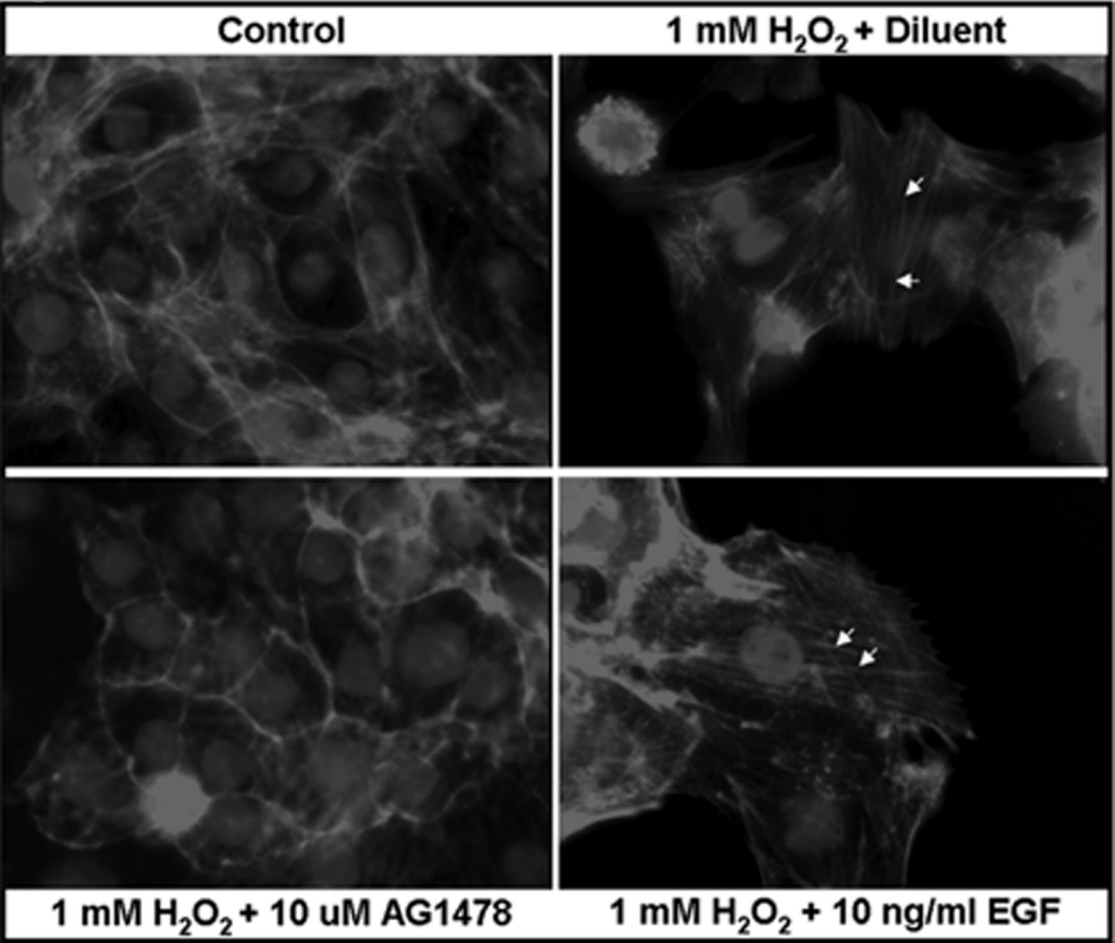
Control
1 mM H_2O_2 + Diluent
1 mM H_2O_2 + 10 uM AG1478
1 mM H_2O_2 + 10 ng/ml EGF

Figure 7

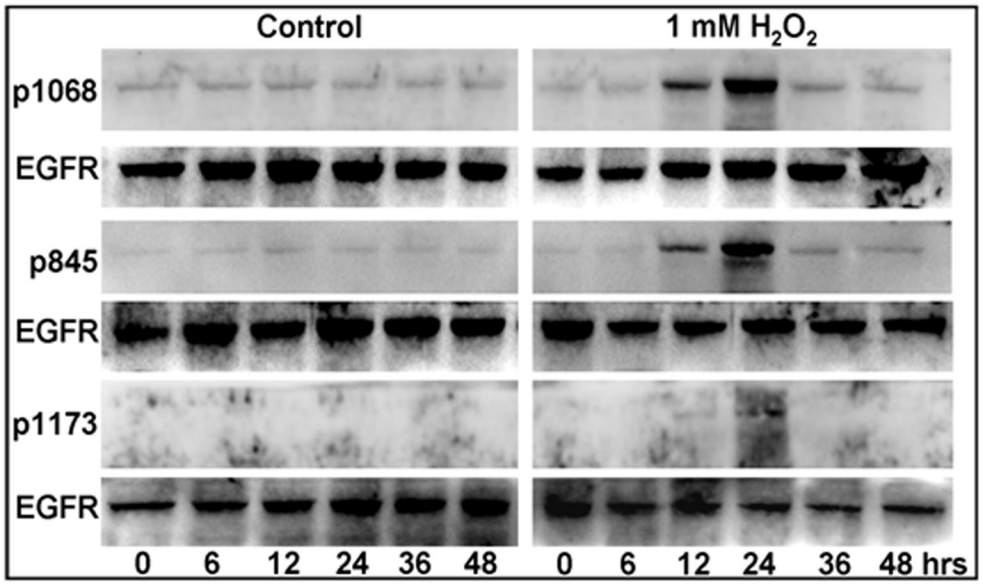

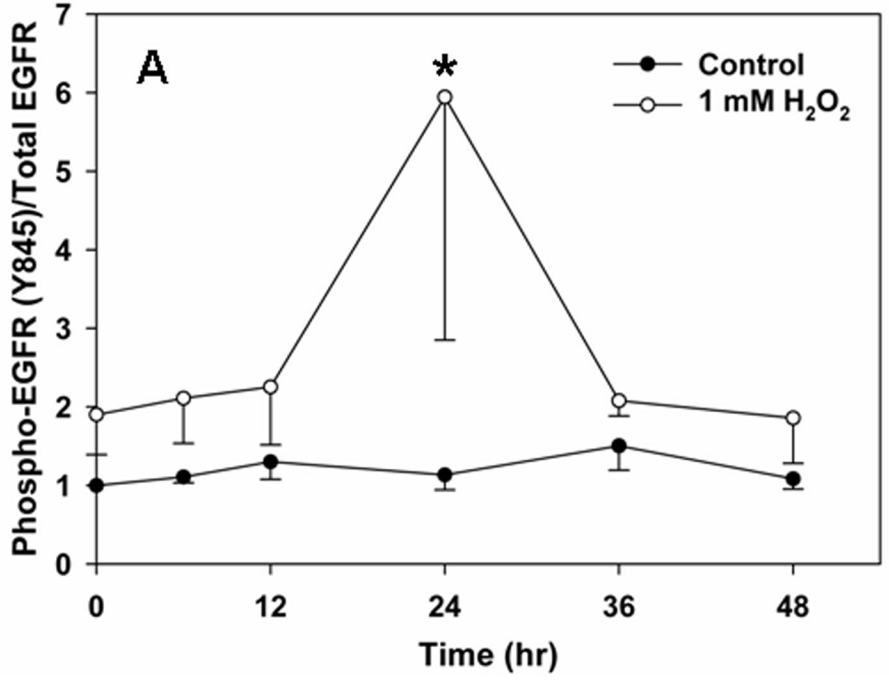

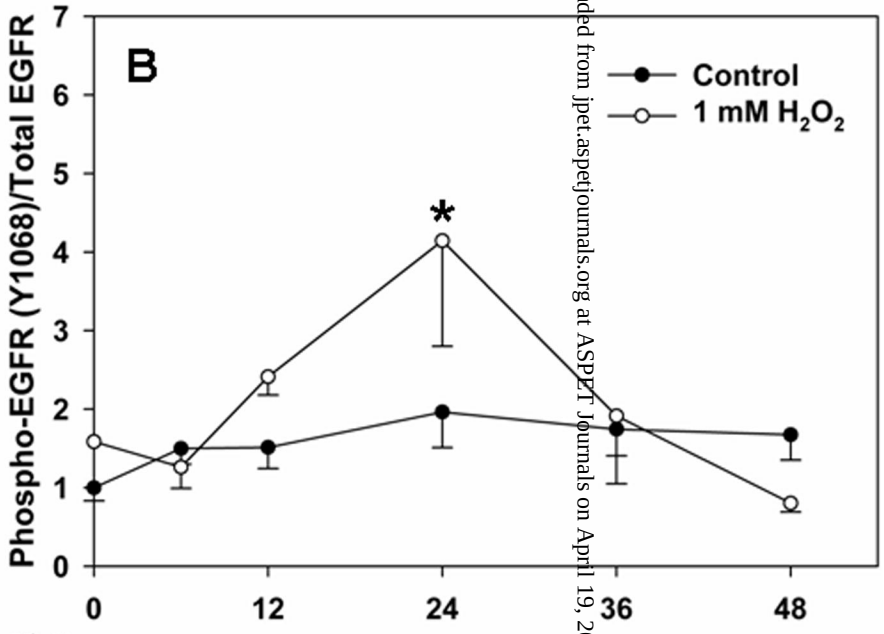

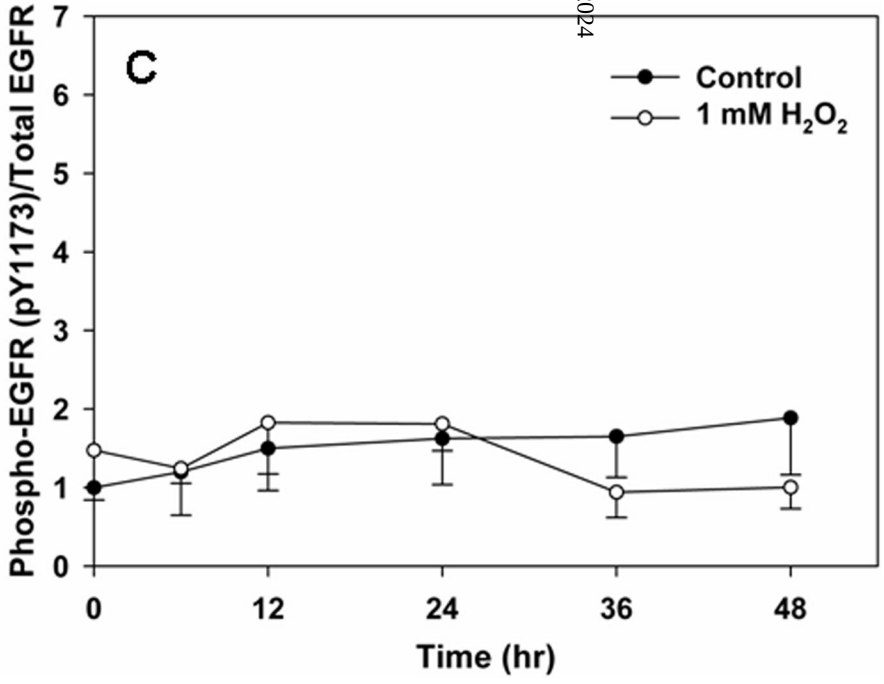

Figure 8

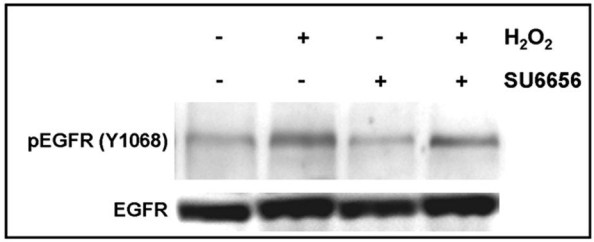
A
- + - + H_2O_2
- - + + SU6656
pEGFR (Y1068)
EGFR

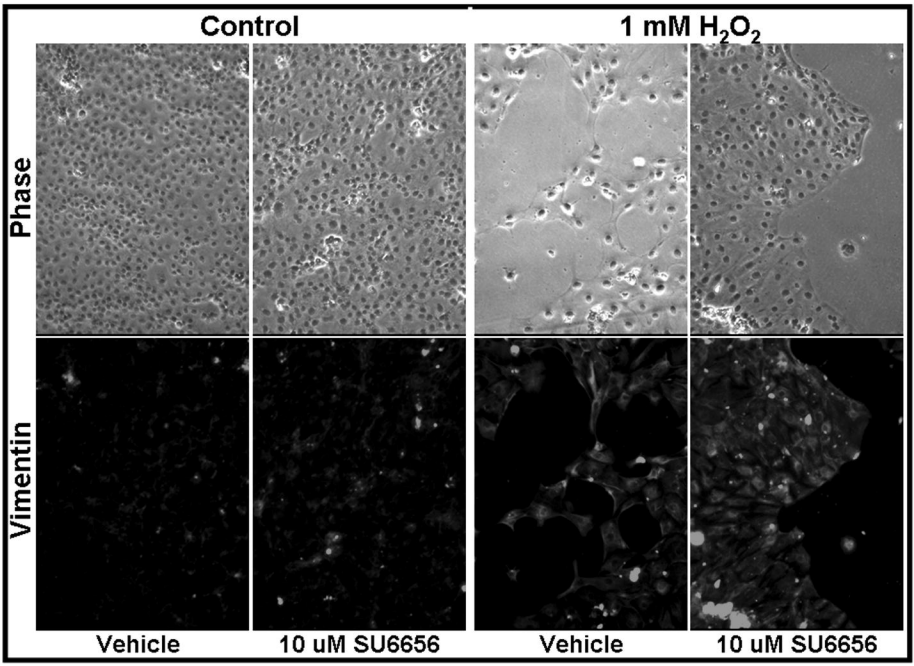
B
Control
1 mM H_2O_2
Phase
Vimentin
Vehicle
10 uM SU6656
Vehicle
10 uM SU6656

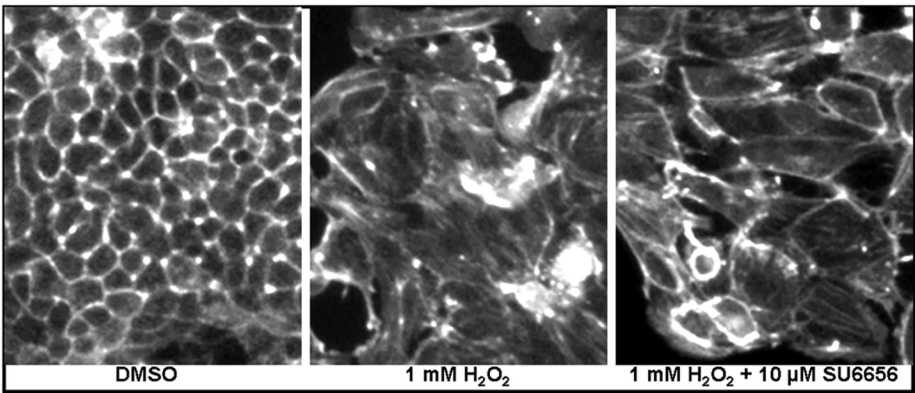
C
DMSO
1 mM H_2O_2
1 mM H_2O_2 + 10 μM SU6656

Figure 9

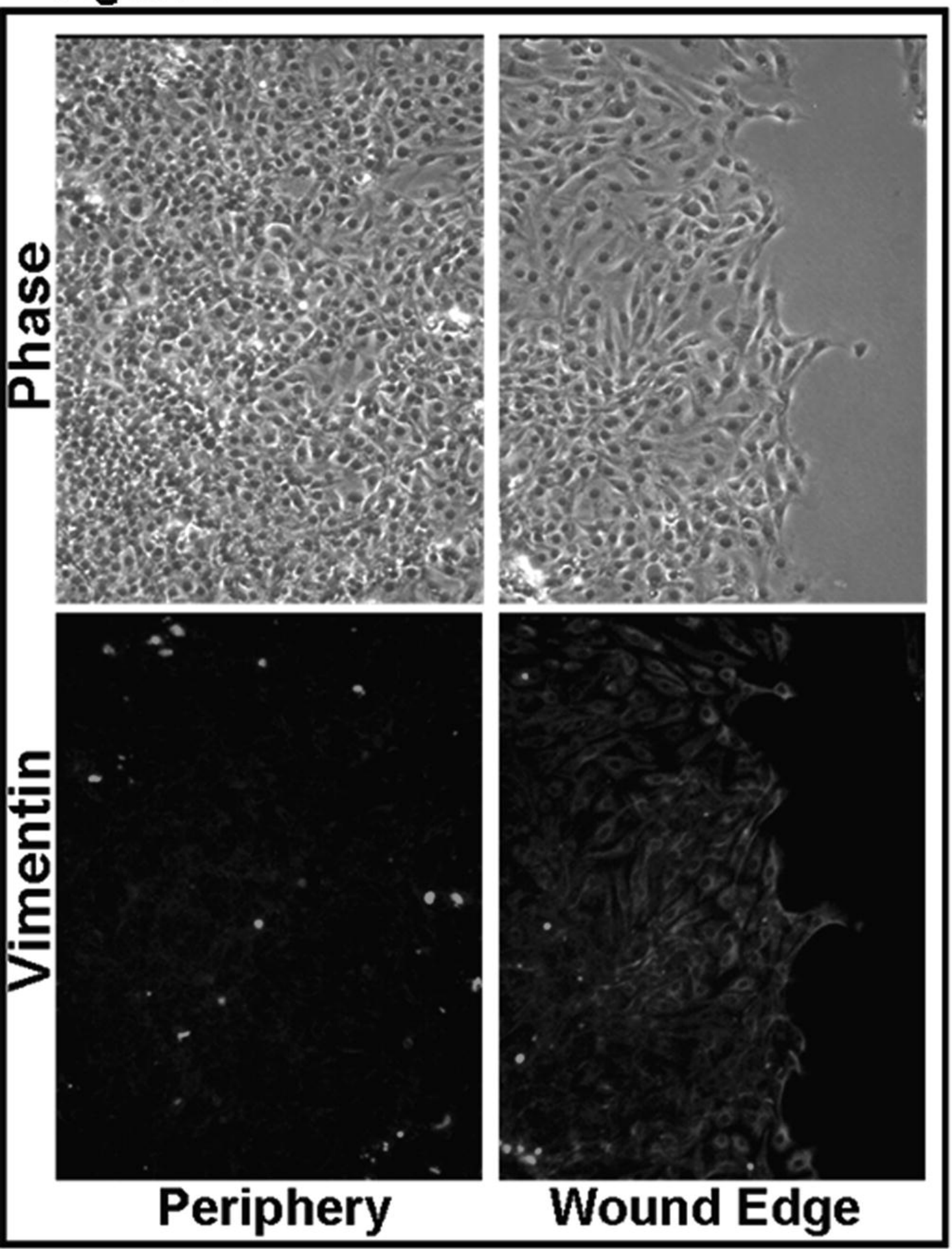

Figure 10

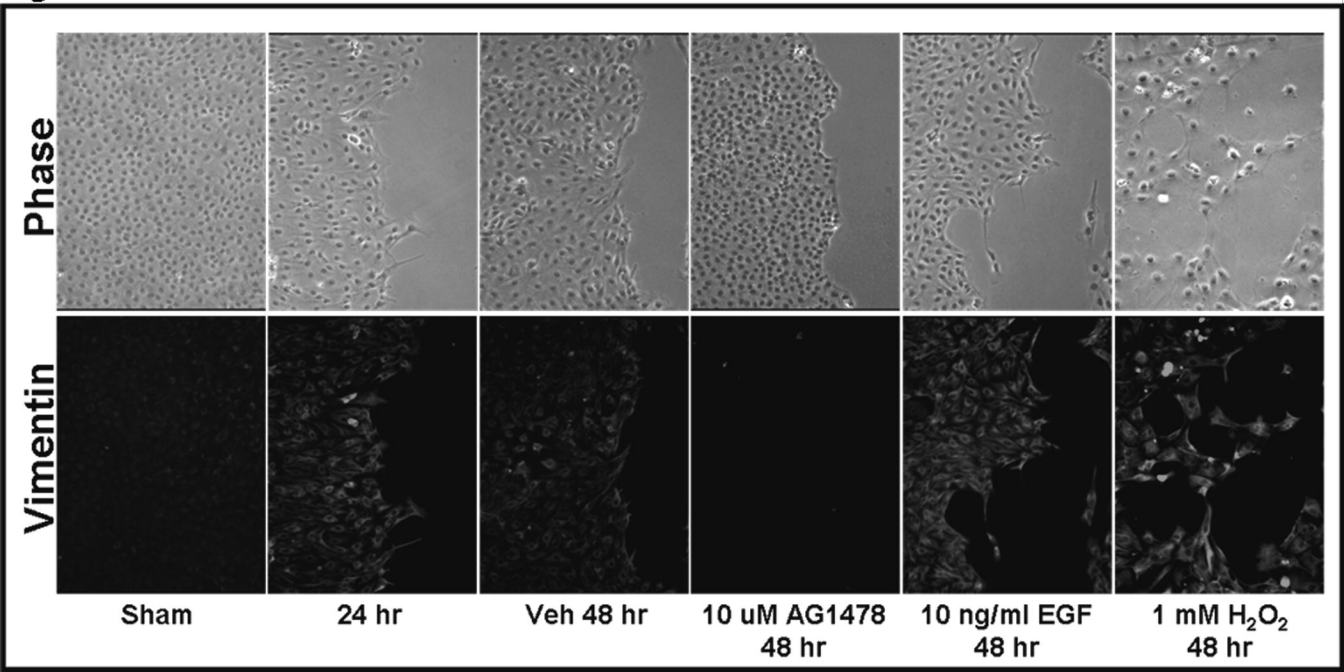
Phase
Vimentin
Sham
24 hr
Veh 48 hr
10 uM AG1478 48 hr
10 ng/ml EGF 48 hr
1 mM H_2O_2 48 hr